

# CP-tagged charm decays: relevance, status and prospects

G. Wilkinson<sup>1</sup>

<sup>1</sup>University of Oxford

## Abstract

The analysis of quantum-correlated  $D - \bar{D}$  decays produced at the  $\psi(3770)$  resonance gives unique insight into quantities such as strong-phase differences and coherence factors. Knowledge of these parameters is invaluable for measurements of the CKM-angle  $\gamma$  ( $\phi_3$ ) in  $B \rightarrow DK$  decays. Results from CLEO-c analyses performed at the  $\psi(3770)$  resonance in a variety of decay channels are reported, and their consequences for the determination of  $\gamma$  is assessed. Future prospects are given for extensions to the present studies.

## Overview

In the last couple of years results have begun to emerge from the  $\psi(3770)$  dataset of the CLEO-c experiment which exploit the quantum-correlated nature of the  $D - \bar{D}$  production at this resonance. These results provide insight into the strong-phase differences existing between  $D^0$  and  $\bar{D}^0$  decays which is of great interest for various applications, in particular the measurement of the CP-violating unitarity triangle angle  $\gamma$  ( $\phi_3$ ) in  $B$ -decays.

This review is organised as follows. First the relevance of CP-tagging is explained, and the basic analysis principle is presented. Results, both preliminary and final, are then shown in two categories of  $D$ -decay:  $D \rightarrow K^0 h^+ h^-$  ( $h = \pi$  or  $K$ )<sup>1</sup> and  $D \rightarrow Kn\pi$  ( $= K^\pm \pi^\mp, K^\pm \pi^\mp \pi^+ \pi^-$  and  $K^\pm \pi^\mp \pi^0$ ). Particular attention is paid to the impact these measurements will have on the determination of  $\gamma$ . Finally, a summary is given, along with future prospects.

## Preliminaries

### Importance of CP-tagged $D$ -decays

CP-tagged  $D$  decays access information which is not available from decays of flavour-tagged mesons, namely the strong-phase difference between  $D^0$  and  $\bar{D}^0$  decay to the final state of interest. As a  $D$ -meson in a CP-eigenstate is a superposition of  $D^0$  and  $\bar{D}^0$ , the decay probability has a dependence on the cosine of this strong-phase difference. In a two-body  $D$ -decay this strong-phase difference is a single quantity, whereas for three or more particles it will vary over Dalitz space, depending on the intermediate resonances contributing at each position.

Knowledge of strong-phase differences (hereafter ‘strong phases’) is important for three reasons.

- It is interesting in itself for understanding  $D$ -decay

dynamics and the resulting light-quark mesons produced.

- It is necessary to relate various measurements of the  $D$ -mixing parameters  $x$  and  $y$  (where  $x$  characterises the mass splitting between the mass eigenstates, and  $y$  the width splitting). For example in the ‘wrong sign’  $D \rightarrow K\pi$  mixing analysis the measured parameters differ from  $x$  and  $y$  through the rotation by the strong phase  $\delta_D^K$ .
- It is invaluable for measurements of the CP-violating angle  $\gamma$  ( $\phi_3$ ).

It is the last point which provides the main context for the discussion in the present review.

### Measuring $\gamma$ in $B \rightarrow DK$ decays

The angle  $\gamma$  is the least well-known parameter of the CKM unitarity triangle with an uncertainty presently estimated to be around  $30^\circ$  [1]. All measurements contributing to our existing knowledge come from the  $B$ -factory experiments, and have been performed using the so-called ‘ $B \rightarrow DK$ ’ family of methods. This approach will continue to dominate the  $\gamma$  determination at the LHCb experiment, where the increased  $B$ -decay statistics will allow an order of magnitude improvement in precision [2].

A  $B^-$  meson may decay to  $D^0 K^-$  through a  $b \rightarrow c$  transition, or  $\bar{D}^0 K^-$  through a  $b \rightarrow u$  transition. If the charm meson is reconstructed in any mode common to both  $D^0$  and  $\bar{D}^0$  (examples include  $K_S^0 \pi^+ \pi^-$  and  $K^\pm \pi^\mp$ ) then interference occurs which involves  $\gamma$ , the CP-violating phase between the two  $b$ -decay paths. Therefore measuring the difference in rates (or kinematical distributions in the case of three-or-more-body channels) between  $B^-$  and  $B^+$  decays gives sensitivity to this angle.

In order to extract  $\gamma$ , however, other parameters must be accounted for which also affect the interference. These include  $r_B$ , the ratio of the magnitude of the  $B$ -decay amplitudes,  $\delta_B$ , the strong-phase difference between the  $B$ -decay amplitudes, and  $\delta_D$  the strong phase (or phases) associated with the  $D$ -decay. Although in some cases it is in principle possible to use the  $B$ -data themselves to extract the  $B$ - and  $D$ -decay parameters along with  $\gamma$ , it is generally advantageous, and often essential, to have an external constraint (or constraints) on  $\delta_D$ . The best source of this information is CP-tagged  $D$ -decays.

### Quantum-correlated $\psi(3770)$ decays

The most practical source of CP-tagged  $D$  decays are neutral  $D - \bar{D}$  events produced at the  $\psi(3770)$  resonance in

<sup>1</sup>In this article  $D$  will be used to indicate any neutral  $D$ -meson.

which one meson (the ‘signal  $D$ ’) decays to the final state of interest, and the other is reconstructed in a CP-eigenstate (the ‘tagging  $D$ ’). The  $D - \bar{D}$  system is produced in a coherent state which, due to the quantum numbers of the resonance, is known to be C-odd. Therefore if one  $D$  is reconstructed as CP-even, for example through  $D \rightarrow K^+K^-$ , then the other meson is ‘tagged’ as being in a CP-odd state.

Reconstructing both  $D$ -mesons (‘double-tagging’) in  $\psi(3770)$  decays allows for studies to be generalised beyond pure CP-tagging. As all hadronic final states can be accessed from both  $D^0$  and  $\bar{D}^0$  decays this means that even if the tagging  $D$  is reconstructed in a non-CP eigenstate hadronic mode then the signal  $D$  will also be in some superposition of  $D^0$  and  $\bar{D}^0$ , albeit not in the equal proportions that are present in the CP-tagged case. Such events turn out to be a powerful addition to the pure CP-tagged sample and are extensively used in the analyses described in this review. For this reason the subsequent discussion will often refer to ‘quantum-correlated decays’.

The only existing  $\psi(3770)$  dataset of significant size was collected by the CLEO-c experiment in  $e^+e^-$  collisions at the Cornell Electron Storage Ring (CESR). CLEO-c finished operation in Spring 2008, by which time it had accumulated  $818 \text{ pb}^{-1}$  of data at the  $\psi(3770)$  resonance, together with additional integrated luminosity at other centre-of-mass energies. All analyses presented in this review use this dataset. In the near future, higher statistics samples are expected from BES-III [3].

There are other important side-benefits to running at this threshold energy of 3770 MeV. Events are very clean, without fragmentation debris. If all  $D$ -decay charged particles and photons are identified in the event, the kinematical constraints allow the presence of neutral particles such as  $K_L^0$  or indeed neutrinos to be inferred. This feature enables the range of CP-tags to be essentially doubled with respect to those available with normal reconstruction techniques. For example  $K_L^0\pi^0$  decays may be used as well as  $K_S^0\pi^0$ . Furthermore, signal decays involving  $K^0$  mesons may be studied in both the  $K_S^0$  and  $K_L^0$  categories.

## Quantum correlated studies of $D \rightarrow K_S^0 h^+ h^-$ decays

### Model dependent measurement of $\gamma$ in $B \rightarrow D(K_S^0\pi^+\pi^-)K$ decays

With the statistics presently available at the  $B$ -factory experiments the highest sensitivity to the angle  $\gamma$  is found in the channel  $B \rightarrow D(K_S^0\pi^+\pi^-)K$ . Comparison of the  $K_S^0\pi^+\pi^-$  Dalitz space in decays originating from a  $B^-$  with those from a  $B^+$  meson reveals CP-violating differences which, when analysed in an unbinned likelihood fit, can be used to extract a value for  $\gamma$ . Using this approach BABAR obtain a result of  $\gamma = (76 \pm 22 \pm 5 \pm 5)^\circ$  [4] and Belle  $\gamma = (76_{-13}^{+12} \pm 4 \pm 9)^\circ$  [5]. Here the uncertainties

are statistical, systematic and model errors, respectively<sup>2</sup>. In fact the BABAR result also receives a contribution from the analysis of  $B \rightarrow D(K_S^0K^+K^-)K$  events; the model error for  $B \rightarrow D(K_S^0\pi^+\pi^-)K$  alone is estimated to be  $\sim 7^\circ$ .

The model uncertainty in these analyses represents the limit in the understanding of the  $D$ -meson decay. The likelihood function used in the fit includes a description of the  $D^0 \rightarrow K_S^0\pi^+\pi^-$  decay which is modelled from a sample of flavour-tagged  $D^{*+} \rightarrow D^0(K_S^0\pi^+\pi^-)\pi^+$  events. Both BABAR and Belle have developed their own models of this decay. The BABAR model, for example, derives from 487,000 events and is based on the isobar formalism [6], with the S-wave  $\pi\pi$  and  $K\pi$  contributions treated with the K-matrix [7] and LASS [8] approaches respectively. The agreement of data with this model is very impressive, but inevitably is not perfect. (The  $\chi^2/n.d.f.$  is found to be 1.11 for  $\sim 19k$  degrees of freedom.) Although a  $7 - 9^\circ$  model uncertainty is at present adequate in the measurement of  $\gamma$  given the  $B$ -meson decay statistics available at the  $B$ -factories, it will rapidly become a limiting factor to the precision of the same analysis performed at LHCb, where a few degree statistical uncertainty is foreseen with  $10 \text{ fb}^{-1}$  [9]. A model independent approach is therefore highly desirable.

### Model independent measurement of $\gamma$ in $B \rightarrow D(K_S^0\pi^+\pi^-)K$ decays

A binned Dalitz analysis approach to the  $\gamma$  determination in  $B \rightarrow D(K_S^0\pi^+\pi^-)K$  [10, 11] removes any model dependence by relating the number of events observed in a given bin of Dalitz space to *experimental observables*. If the Dalitz plot is partitioned into a set of bins symmetric through the line  $m^2(K_S^0\pi^+) = m^2(K_S^0\pi^-)$ , then the number of  $B^\pm$  events giving rise to decays in bin  $i$  is given by:

$$N_i^\pm = h \left( K_i + r_B^2 K_{-i} + 2\sqrt{K_i K_{-i}}(x_\pm c_i \pm y_\pm s_i) \right) \quad (1)$$

where  $h$  is a normalisation factor,  $x_\pm = r_B \cos(\delta_B \pm \gamma)$ ,  $y_\pm = r_B \sin(\delta_B \pm \gamma)$ ,  $K_i$  are the number of flavour-tagged  $D^0 \rightarrow K_S^0\pi^+\pi^-$  decays in bin  $i$ , and  $c_i$  and  $s_i$  are the amplitude averaged cosine and sine of the strong phase of the  $D$ -decay in the bin in question. In this expression the subscript  $-i$  indicates a bin which is defined symmetrically in the lower region of the Dalitz plot with respect to bin  $i$  in the upper region. The parameters  $\gamma$ ,  $r_B$  and  $\delta_B$  are to be extracted from the measurement, while  $c_i$  and  $s_i$  are inputs which are determined from quantum-correlated  $D$ -decays. The values of  $K_i$  can be determined from any sample of flavour-tagged  $D$ -decays.

In making such a measurement the statistical sensitivity is affected by the choice of binning. It is advantageous to

<sup>2</sup> It may be noted that there is a significant difference in the reported statistical precision in the two results which cannot be explained by the variation in sample sizes between the experiments. This difference is largely driven by the very different values of the interference parameter  $r_B$  that is found in the two analyses.

define bins in which the variation of strong phase is small (so that  $c_i^2 + s_i^2$  is as close as possible to 1). This choice can be informed by the models developed on the flavour-tagged data. It must be emphasised, however, that any difference between the model and reality will *not* lead to any bias in the measurement, but will merely result in the statistical sensitivity being lower than expected. In the analysis reported below 8 bins are chosen, each covering the same span in strong phase. The model used to make this choice is that constructed by BABAR [4]. This binning is shown in Fig. 1.

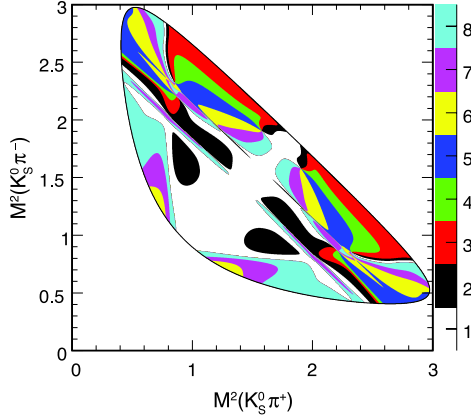


Figure 1: Equal phase binning of the  $D^0 \rightarrow K_S^0 \pi^+ \pi^-$  Dalitz plot.

### Measurement of $c_i$ and $s_i$ in $D \rightarrow K_S^0 \pi^+ \pi^-$

The parameters  $c_i$  and  $s_i$  have been determined using  $818 \text{ fb}^{-1}$  of  $\psi(3770)$  data collected by CLEO-c [12]. Central to the analysis is a sample of double-tagged events in which  $D \rightarrow K_S^0 \pi^+ \pi^-$  decays are reconstructed together with a CP-eigenstate, or against other  $D \rightarrow K_S^0 \pi^+ \pi^-$  decays.  $D \rightarrow K_L^0 \pi^+ \pi^-$  decays are also used. The presence of a  $K_L^0$  mesons is inferred by selecting events in which the missing-mass squared is consistent with  $m_{K_L^0}^2$ , as illustrated in Fig. 2

A summary of the double-tag sample is given in Tab. 1. Four CP-even tag and three CP-odd tag modes are employed alongside  $D \rightarrow K_S^0 \pi^+ \pi^-$  decays. Background considerations mean that certain CP-tags are not used with the  $D \rightarrow K_L^0 \pi^+ \pi^-$  decays. Approximately 1600 CP-tagged events are selected in total, and around 1300  $K_S^0 \pi^+ \pi^-$  vs  $K^0 \pi^+ \pi^-$  events. The signal to background level is between 10 and 100, depending on the tag mode. Also selected (but not tabulated here) are events in which the signal is reconstructed alongside decays such as  $D \rightarrow K^\pm \pi^\mp$ , which to a very good approximation serve as flavour-tags.

An inspection of the Dalitz plots and projections for the CP-tagged  $K_S^0 \pi^+ \pi^-$  samples, as presented in Fig. 3, reveals clear differences. For example, the sample with the CP-even tags has in the  $m^2(\pi^+ \pi^-)$  projection a clear  $\rho^0$

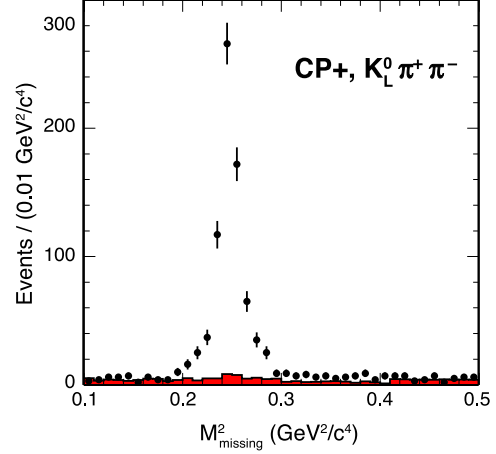


Figure 2: CLEO-c missing mass squared distribution in  $K_L^0 \pi^+ \pi^-$  events reconstructed together with CP-even tags. The shaded histogram represents the background expectation from the simulation.

Table 1: CLEO-c double tag yields in the  $K^0 \pi^+ \pi^-$  analysis.

Mode	$K_S^0 \pi^+ \pi^-$ yield	$K_L^0 \pi^+ \pi^-$ yield
CP-even tags		
$K^+ K^-$	124	345
$\pi^+ \pi^-$	62	172
$K_S^0 \pi^0 \pi^0$	56	-
$K_L^0 \pi^0$	229	-
CP-odd tags		
$K_S^0 \pi^0$	189	281
$K_S^0 \eta$	39	41
$K_S^0 \omega$	83	-
Other tags		
$K_S^0 \pi^+ \pi^-$	475	867

peak associated with the CP-odd  $K_S^0 \rho$  decays. This feature is absent from the sample with the CP-odd tags. The corresponding  $K_L^0 \pi^+ \pi^-$  distributions are shown in Fig. 4. Observe that, as expected, the  $K_L^0 \pi^+ \pi^-$  with CP-even(-odd) tag distributions resemble those of the  $K_S^0 \pi^- \pi^+$  with CP-odd(-even) tags.

In the analysis the parameters  $c_i$  and  $s_i$  are determined from measuring the event yield, after background subtraction and efficiency correction, in each bin of the Dalitz plot for the CP-tagged and the  $K_S^0 \pi^+ \pi^-$  vs  $K^0 \pi^+ \pi^-$  samples. The number of events in bin  $i$  of a CP-tagged  $K_S^0 \pi^+ \pi^-$  Dalitz plot is

$$M_i^\pm = h_{CP^\pm} \left( K_i \pm 2c_i \sqrt{K_i K_{-i}} + K_{-i} \right) \quad (2)$$

where  $h_{CP^\pm}$  is a normalisation factor which can be determined from the number of single flavour-tagged signal decays and single CP-decays. For a  $K_S^0 \pi^+ \pi^-$  vs  $K_S^0 \pi^+ \pi^-$

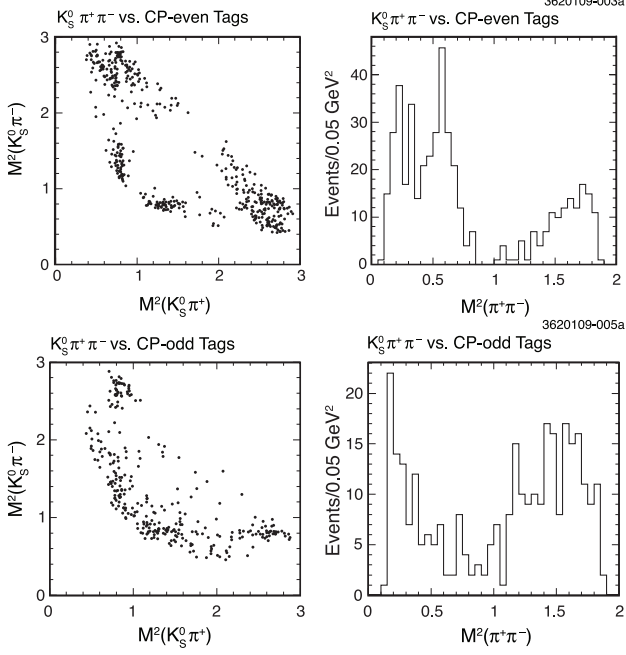


Figure 3: CLEO-c Dalitz plots and projections for CP-tagged  $K_S^0 \pi^+ \pi^-$  events.

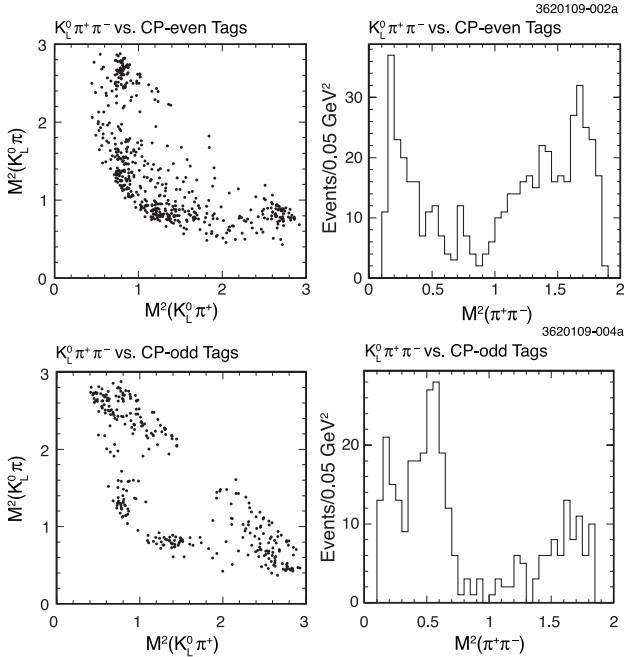


Figure 4: CLEO-c Dalitz plots and projections for CP-tagged  $K_L^0 \pi^+ \pi^-$  events.

sample, the number of events with entries in bin  $i$  of the first plot and bin  $j$  of the second plot is given by

$$M_{ij} = h_{corr}(K_i K_{-j} + K_{-i} K_j - 2\sqrt{K_i K_{-j} K_{-i} K_j}(c_i c_j + s_i s_j)) \quad (3)$$

where  $h_{corr}$  is another normalisation factor.

Events including  $D^0 \rightarrow K_L^0 \pi^+ \pi^-$  decays make a sig-

nificant contribution to the overall sensitivity of the analysis. Superficially, CP-even (-odd)  $K_L^0 \pi^+ \pi^-$  events can be treated as CP-odd (-even)  $K_S^0 \pi^+ \pi^-$  events. The expression for the number of CP-tagged  $K_L^0 \pi^+ \pi^-$  events in bin  $i$  is given by

$$M_i^\pm = h_{CP\pm} \left( K_i \mp 2c_i' \sqrt{K_i K_{-i}} + K_{-i} \right) \quad (4)$$

and the corresponding expression to Eqn. 3 for  $K_S^0 \pi^+ \pi^-$  vs  $K_L^0 \pi^+ \pi^-$  decays is

$$M_{ij} = h_{corr}(K_i K_{-j} + K_{-i} K_j + 2\sqrt{K_i K_{-j} K_{-i} K_j}(c_i c_j' + s_i s_j')). \quad (5)$$

As well as the sign-flips with respect to the earlier expressions, note that the cosine and sine of the binned strong phases for the  $D \rightarrow K_L^0 \pi^+ \pi^-$  decays are denoted with the primed quantities  $c_i'$  and  $s_i'$ . These are not expected to be quite identical to  $c_i$  and  $s_i$ , as can be seen by writing

$$A(D^0 \rightarrow K_S^0 \pi^+ \pi^-) = \frac{1}{\sqrt{2}} [A(D^0 \rightarrow \bar{K}^0 \pi^+ \pi^-) + A(D^0 \rightarrow K^0 \pi^+ \pi^-)]$$

and

$$A(D^0 \rightarrow K_L^0 \pi^+ \pi^-) = \frac{1}{\sqrt{2}} [A(D^0 \rightarrow \bar{K}^0 \pi^+ \pi^-) - A(D^0 \rightarrow K^0 \pi^+ \pi^-)],$$

from which it follows

$$A(D^0 \rightarrow K_L^0 \pi^+ \pi^-) = A(D^0 \rightarrow K_S^0 \pi^+ \pi^-) - \sqrt{2} A(D^0 \rightarrow K^0 \pi^+ \pi^-).$$

Thus in relating  $D^0 \rightarrow K_L^0 \pi^+ \pi^-$  to  $D^0 \rightarrow K_S^0 \pi^+ \pi^-$  the set of doubly Cabibbo suppressed (DCS) amplitudes  $A(D^0 \rightarrow K^0 \pi^+ \pi^-)$  appear as a correction term, with a minus sign.

If, for the purposes of illustration, we consider only intermediate resonances of the sort  $K^{*\pm}$  and  $\rho^0$  then it is easy to show

$$A(D^0 \rightarrow K_S^0 \pi^+ \pi^-) = \alpha K^{*-} \pi^+ + \beta K^{*+} \pi^- + \chi \rho^0 K_S^0 \quad (6)$$

and

$$A(D^0 \rightarrow K_L^0 \pi^+ \pi^-) = \alpha K^{*-} \pi^+ - \beta K^{*+} \pi^- + \chi' \rho^0 K_L^0, \quad (7)$$

where  $\alpha$ ,  $\beta$ ,  $\chi$  and  $\chi'$  are coefficients. Thus in going from  $K_S^0 \pi^+ \pi^-$  to  $K_L^0 \pi^+ \pi^-$  the  $K^{*+} \pi^-$  term changes sign, and the  $\rho^0$  term enters with a different factor, which is caused by the sign-flip in the DCS contribution to this amplitude. Therefore it is expected that  $c_i' \neq c_i$  and  $s_i' \neq s_i$ , although the difference between the two sets of parameters is predicted to be small.

In the analysis  $c_i$ ,  $s_i$ ,  $c_i'$  and  $s_i'$  are extracted simultaneously, but the allowed differences between the unprimed

and primed quantities are constrained in the fit. The expected differences on which this constraint is based are calculated from the flavour-tagged models of the  $K_S^0\pi^+\pi^-$  decay, which give the coefficients  $\alpha$ ,  $\beta$  and  $\chi$ . The coefficient  $\chi'$  is related to  $\chi$  by a DCS correction, the phase and magnitude of which is allowed to vary in a conservative range as a systematic in the study. Additional contributions to the systematic uncertainty come from using different models to give the values of  $\alpha$ ,  $\beta$  and  $\chi$ . The results of these studies indicate that the residual model dependence is small compared with the statistical uncertainty of the analysis.

### Results and impact on the $\gamma$ measurement

The results of the CLEO-c analysis for  $c_i$  and  $s_i$  are shown in Fig. 5, together with the expectations from the BABAR model [4]. The measurement errors are the sum in quadrature of statistical uncertainties, uncertainties arising from the reconstruction (such as that arising from the momentum resolution), and the uncertainties arising from the residual model dependence in the  $K_S^0\pi^+\pi^- - K_L^0\pi^+\pi^-$  constraint. The statistical uncertainties are dominant. The  $c_i$  measurements are more precise than those from  $s_i$ , as they benefit both from the CP-tags and the  $K^0\pi^+\pi^-$  vs  $K^0\pi^+\pi^-$  events, whereas sensitivity to  $s_i$  comes solely from the latter category. The measurements are compatible with the model predictions.

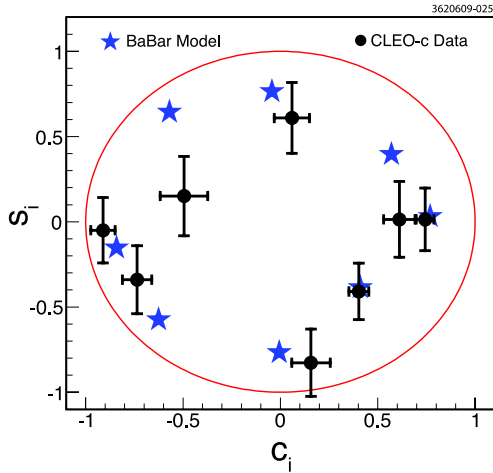


Figure 5: CLEO-c results [12] and model predictions [4] for  $c_i$  and  $s_i$ .

When these results for  $c_i$  and  $s_i$  will be used as input to the  $\gamma$  determination using  $B \rightarrow D(K_S^0\pi^+\pi^-)K$  decays, the uncertainties on the parameter values will induce a corresponding error on  $\gamma$ . This uncertainty has been estimated to be around  $2^\circ$ , which is much smaller than both the present BABAR assigned model uncertainty of  $7^\circ$  and the expected statistical uncertainty of  $5.5^\circ$  at LHCb with  $10 \text{ fb}^{-1}$ . The loss in statistical precision from the binned method, compared with a binned model-dependent approach, is a relative 20%. It is being investigated whether

an alternative choice of binning could reduce this loss. With the present binning the sensitivity to  $\gamma$  will surpass that of the unbinned approach with less than  $2 \text{ fb}^{-1}$  of LHCb data.

### Extending to $D \rightarrow K_S^0 K^+ K^-$

As has been demonstrated by BABAR [4],  $B \rightarrow D(K_S^0 K^+ K^-)K$  decays can be used to measure  $\gamma$  using a model dependent unbinned fit with a method entirely analogous to that used for  $B \rightarrow D(K_S^0\pi^+\pi^-)K$ . In order to allow a model independent exploitation of this mode, CLEO-c has embarked upon a measurement of the corresponding  $c_i$  and  $s_i$  parameters in  $D \rightarrow K_S^0 K^+ K^-$ . This determination will exploit around 550 quantum-correlated double tags, including  $K^0 K^+ K^-$  vs  $K^0\pi^+\pi^-$  events that can contribute to the analysis thanks to the knowledge of the  $c_i$  and  $s_i$  values for  $D \rightarrow K_S^0\pi^+\pi^-$ .

Figure 6 shows the Dalitz plots and  $m^2(K^+K^-)$  projections for CP-tagged  $K_S^0 K^+ K^-$  and  $K_L^0 K^+ K^-$  events. Observe that the  $\phi$  peak associated with  $K_{S(L)}^0\phi$  decays is only prominent for the CP-even(odd) tags.

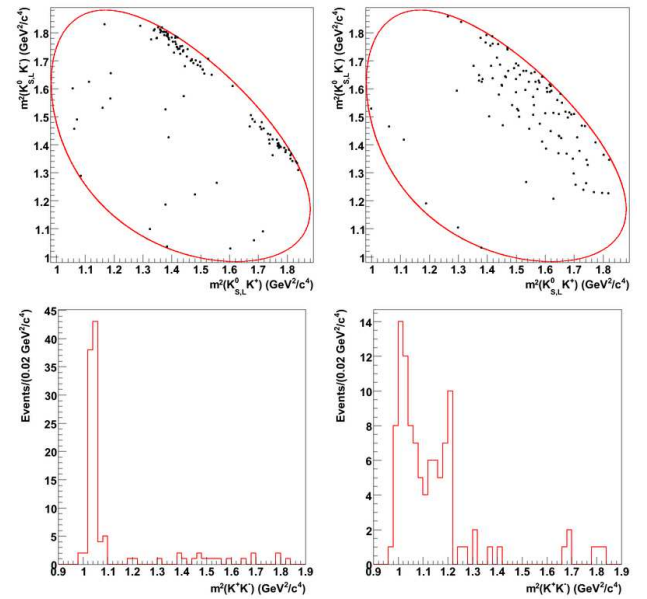


Figure 6: CLEO-c  $D \rightarrow K^0 K^+ K^-$  Dalitz plots and projections. Left:  $K_{S(L)}^0 K^+ K^-$  with CP-even(odd) tags. Right:  $K_{S(L)}^0 K^+ K^-$  with CP-odd(even) tags.

Preliminary results on the measurement of the strong phase difference in  $D \rightarrow K_S^0 K^+ K^-$  events can be found in [13].

### Quantum correlated studies of $D \rightarrow K(n)\pi$ decays

#### The ADS strategy for measuring $\gamma$

A powerful subset of the  $B \rightarrow DK$  family of methods to measure  $\gamma$  is the so-called ‘ADS’ approach [14]. Here the  $D$ -decay mode that is reconstructed is one which involves a charged kaon and one or more pions. The simplest

example is  $D \rightarrow K^\pm \pi^\mp$ , which is here taken as an example. Depending on the charge of the  $B$ -meson and the kaon from the  $D$ -decay, there are four possible final states. The partial widths into each state depend on the physics parameters of interest. Two of these final states have particular sensitivity:

$$\Gamma(B^\mp \rightarrow (K^\pm \pi^\mp)_D K^\mp) \propto r_B^2 + (r_D^{K\pi})^2 + 2r_B r_D^{K\pi} \cos(\delta_B + \delta_D^{K\pi} \mp \gamma). \quad (8)$$

Since  $r_B$  and the magnitude of the ratio between the doubly Cabibbo suppressed and the favoured  $D$  decay amplitudes,  $r_D^{K\pi}$ , are of similar size, the interference term that involves  $\gamma$  appears at first order. The consequence is that a large asymmetry may exist between the number of events found in each final state. Measuring this asymmetry, and combining with observables in other  $B \rightarrow DK$  modes, allows  $\gamma$  to be determined. This extraction however benefits from external constraints on the  $D$ -decay parameters  $r_D^{K\pi}$  and  $\delta_D^{K\pi}$ . The former of these is well known, essentially from the ratio of the suppressed and favoured branching ratios. Knowledge of  $\delta_D^{K\pi}$  comes both from  $\psi(3770)$  decays and from the ensemble of  $D$ -meson mixing measurements, as is discussed below.

The form of the ADS decay rates, given in expression 8, takes on a different form for multibody decays such as  $D \rightarrow K^\pm \pi^\mp \pi^+ \pi^-$ . In this case there are many intermediate resonances (eg.  $K^{*0} \rho^0$ ,  $K^\pm a_1^\mp$ ), which in general will contribute with different strong phases. The two rates of interest are then as follows:

$$\Gamma(B^\mp \rightarrow (K^\pm \pi^\mp \pi^- \pi^+)_D K^\mp) \propto r_B^2 + (r_D^{K3\pi})^2 + 2r_B r_D^{K3\pi} R_{K3\pi} \cos(\delta_B + \delta_D^{K3\pi} \mp \gamma). \quad (9)$$

The parameter  $R_{K3\pi}$  is termed the coherence factor, and can take any value between 0 and 1, where the latter limit corresponds to the case when all resonances contribute in phase and the channel behaves as a two-body decay. The parameter  $\delta_D^{K3\pi}$  is now the strong-phase difference averaged over all Dalitz space. Precise definitions of the quantities can be found in [15]. Analogous parameters exist for other decays, for example  $R_{K\pi\pi^0}$  and  $\delta_D^{K\pi\pi^0}$  in the case of  $D \rightarrow K^\pm \pi^\mp \pi^0$ .

### Analysis of the mode $D \rightarrow K^\pm \pi^\mp$

The strong-phase difference  $\delta_D^{K\pi}$  between  $D^0$  and  $\bar{D}^0$  decays to  $K^+ \pi^-$  has been determined by CLEO-c using 281 pb<sup>-1</sup> of  $\psi(3770)$  data [16]. This result is the least recent of those reported in this review, and so only a very brief summary of the analysis is given here.

If one neglects mixing then the rate,  $F_{CP^\pm}^{K\pi}$ , of CP-tagged  $D \rightarrow K^\pm \pi^\mp$  events is as follows:

$$F_{CP^\pm}^{K\pi} \approx \mathcal{B}_{CP^\pm} \mathcal{B}_{K\pi} (1 + (r_D^{K\pi})^2 \pm 2r_D^{K\pi} \cos \delta_D^{K\pi}). \quad (10)$$

where  $\mathcal{B}_{CP^\pm}$  and  $\mathcal{B}_{K\pi}$  are the branching ratios of the CP-tag and the Cabibbo favoured signal decay, respectively.

The analysis reported in [16] uses a range of CP-tags, other double-tagged events, and single tags both to extract  $\delta_D^{K\pi}$  and to gain sensitivity to the mixing parameters  $x$  and  $y$ , which modify the result for  $F_{CP^\pm}^{K\pi}$  and the rates for other event types.

When a fit is performed which imposes no external constraints on the mixing parameters, a result for the strong phase difference of  $\cos \delta_D^{K\pi} = 1.03_{-0.17}^{+0.31} \pm 0.06$  is obtained<sup>3</sup>. In fact this measurement is less precise than that of the indirect determination which can be obtained from a global fit to all the  $D$ -mixing results [17]. As Fig. 7 makes clear, however, the inclusion of the CLEO-c result brings important extra information, as it resolves a two-fold ambiguity which would otherwise exist in our knowledge of  $\delta_D^{K\pi}$ .

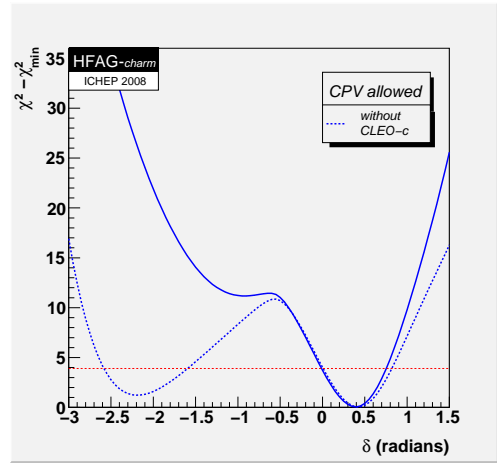


Figure 7: CLEO-c impact on the knowledge of  $\delta_D^{K\pi}$  [17]. The dotted line is obtained from a global fit to  $D$ -mixing measurements which do not use  $\psi(3770)$  data and the solid line from a fit which in addition includes the result of [16].

This analysis is now being updated with the full CLEO-c dataset and improved analysis methods [18].

### Analysis of the modes $D \rightarrow K^\pm \pi^\mp \pi^+ \pi^-$ and $D \rightarrow K^\pm \pi^\mp \pi^0$

The coherence factors and the average strong phase differences have been determined by CLEO-c for the modes  $D \rightarrow K^\pm \pi^\mp \pi^+ \pi^-$  and  $D \rightarrow K^\pm \pi^\mp \pi^0$  using 818 fb<sup>-1</sup> of  $\psi(3770)$  data [19]. The analysis is based on the method proposed in [15]. Each signal mode is reconstructed alongside various categories of tags. These include: CP-eigenstates; the signal mode itself in the case where the two kaons in the event are of identical sign (giving so-called

<sup>3</sup>It is worth remarking that the convention used to describe the effect of a CP operation on the  $D^0$  meson has non-trivial consequences in the definition of phase differences. In particular, the convention assumed in most charm mixing analyses, and implicit in the results presented here, is offset by  $\pi$  from that assumed in most  $B \rightarrow DK$  studies. Thus the central value that should be used in both expressions 8 and 9 is *not*  $\delta_D^{K\pi} \approx 0.4$ , as suggested by Fig. 7, but  $\delta_D^{K\pi} \approx 0.4 - \pi$ .

Table 2: Dependence of double-tag rates in the coherence factor analysis.

Double-tag	Sensitive to
$K^\pm\pi^\mp\pi^+\pi^-$ vs $K^\pm\pi^\mp\pi^+\pi^-$	$(R_{K3\pi})^2$
$K^\pm\pi^\mp\pi^0$ vs $K^\pm\pi^\mp\pi^0$	$(R_{K\pi\pi^0})^2$
$K^\pm\pi^\mp\pi^+\pi^-$ vs CP	$R_{K3\pi} \cos(\delta_D^{K3\pi})$
$K^\pm\pi^\mp\pi^0$ vs CP	$R_{K\pi\pi^0} \cos(\delta_D^{K\pi\pi^0})$
$K^\pm\pi^\mp\pi^+\pi^-$ vs $K^\pm\pi^\mp$	$R_{K3\pi} \cos(\delta_D^{K3\pi} - \delta_D^{K\pi})$
$K^\pm\pi^\mp\pi^0$ vs $K^\pm\pi^\mp$	$R_{K\pi\pi^0} \cos(\delta_D^{K\pi\pi^0} - \delta_D^{K\pi})$
$K^\pm\pi^\mp\pi^+\pi^-$ vs $K^\pm\pi^\mp\pi^0$	$R_{K3\pi} R_{K\pi\pi^0} \cos(\delta_D^{K3\pi} - \delta_D^{K\pi\pi^0})$

Table 3: CLEO-c double-tag background subtracted yields in the coherence factor analysis analysis.

Tag Mode	$K^\pm\pi^\mp\pi^+\pi^-$ yield	$K^\pm\pi^\mp\pi^0$ yield
CP-even tags		
$K^+K^-$	536	764
$\pi^+\pi^-$	246	336
$K_S^0\pi^0\pi^0$	283	406
$K_L^0\pi^0$	695	1234
$K_L^0\omega$	296	449
CP-odd tags		
$K_S^0\pi^0$	705	891
$K_S^0\omega$	319	389
$K_S^0\phi$	53	91
$K_S^0\eta$	164	152
$K_S^0\eta'$	36	61
Other tags		
$K^\pm\pi^\mp\pi^+\pi^-$	29	64
$K^\pm\pi^\mp\pi^0$	see row above	13
$K^\pm\pi^\mp$	36	7

‘like-sign’ events); the other signal mode under consideration, again in the like-sign configuration; and like-sign  $K^\pm\pi^\mp$  decays. The sensitivity of each event class to the coherence factors and strong phase differences is indicated in Tab. 2, although Ref. [15] should be consulted to obtain the complete expressions.

The analysis uses 10 types of CP-tags. The event yield for each category of event, after background subtraction, is listed in Tab. 3. Additional double-tags, not detailed here, include ‘unlike-sign’ events, and  $K^\pm\pi^\mp$  vs CP-eigenstate events, both needed for normalisation purposes.

The analysis chooses as observables so-called ‘ $\rho$ -parameters’, which give the ratio of the number of observed events in each category to the number expected were the  $D - \bar{D}$  pair to decay in an uncorrelated manner, and/or the coherence parameter to be zero. The value of  $\rho_{CP}$ , this ratio for the CP-tagged events, is shown for each CP-tag in Fig. 8. For a given signal-mode the same behaviour is expected for each CP-eigenvalue, and behaviour of an opposite sign for CP-odd and CP-even. The values of the observables are consistent with these expectations.

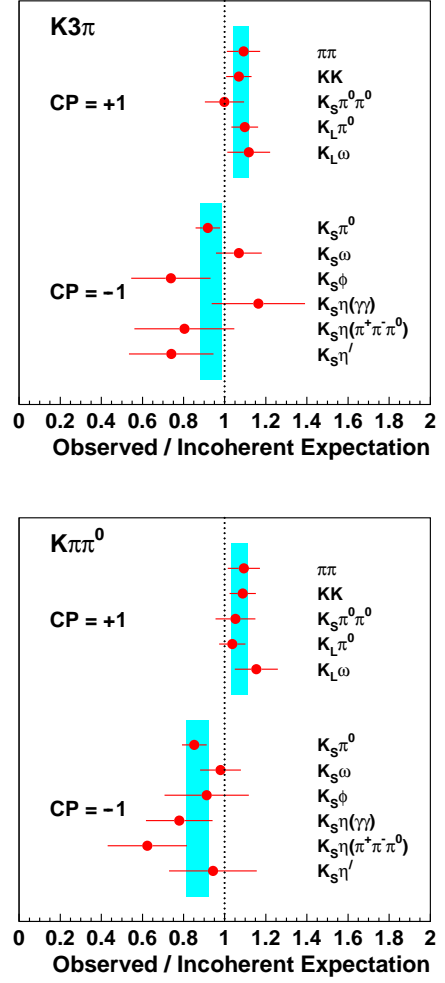


Figure 8: CLEO-c  $\rho_{CP}$  parameters for the  $D \rightarrow K^\pm\pi^\mp\pi^+\pi^-$  (top) and  $D \rightarrow K^\pm\pi^\mp\pi^0$  (bottom) analyses, representing the number of observed events to the incoherent expectation. The cyan shaded bands show the mean result for each CP-eigenvalue.

In Fig. 9 are shown the results for the nine observables. These comprise: the mean results per CP-tag per mode ( $\rho_{CP+}$  and  $\rho_{CP-}$ ); the results for the like-sign events for both signal modes ( $\rho_{LS}$ ); the results for the like-sign  $K\pi$  tags ( $\rho_{K\pi,LS}$ ); and that coming from the like-sign  $K^\pm\pi^\mp\pi^+\pi^-$  vs  $K^\pm\pi^\mp\pi^0$  events ( $\rho_{K3\pi,LS}^{K\pi\pi^0}$ ). The error bars include the statistical and systematic uncertainties. In the case of  $\rho_{CP\pm}$  the largest systematic uncertainty is associated with the normalisation procedure, which is significant alongside the statistical uncertainty, but is itself statistical in origin. For the other observables the systematic uncertainties are small.

The expected size and sign of any deviation of the  $\rho$  parameters from a value of one depends on the tag-category. The general behaviour in Fig. 9, however, makes clear that there is evidence of high coherence in  $D \rightarrow K^\pm\pi^\mp\pi^0$  decays, but much less so for  $D \rightarrow K^\pm\pi^\mp\pi^+\pi^-$ .

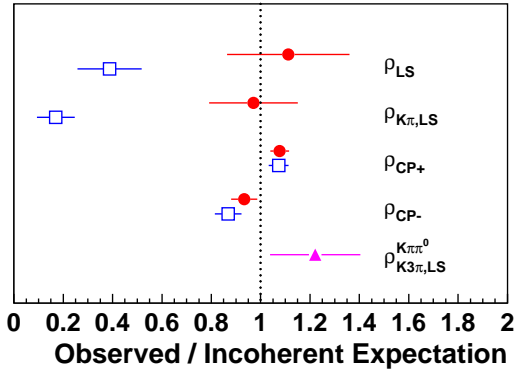


Figure 9: CLEO-c results for coherence observables. Filled red circles indicate  $D \rightarrow K^\pm \pi^\mp \pi^+ \pi^-$ , open blue squares indicate  $D \rightarrow K^\pm \pi^\mp \pi^0$  and the filled magenta triangle indicates like-sign  $K^\pm \pi^\mp \pi^+ \pi^-$  vs  $K^\pm \pi^\mp \pi^0$  events.

Values for the coherence factors,  $R_{K3\pi}$  and  $R_{K\pi\pi^0}$ , and mean strong-phase differences,  $\delta_D^{K3\pi}$  and  $\delta_D^{K\pi\pi^0}$ , have been obtained by making a  $\chi^2$  fit to the above observables. Other free parameters in the fit include  $\delta_D^{K\pi}$ , the mixing parameters  $x$  and  $y$  and the Cabibbo favoured and doubly suppressed branching ratios, all of which are given a Gaussian constraint to lie close to their world-best measured values. The best fit values for the coherence factors and strong phases are as follows:  $R_{K3\pi} = 0.33_{-0.23}^{+0.20}$ ,  $R_{K\pi\pi^0} = 0.84 \pm 0.07$ ,  $\delta_D^{K3\pi} = (114_{-23}^{+26})^\circ$  and  $\delta_D^{K\pi\pi^0} = (227_{-17}^{+14})^\circ$ . The one, two and three sigma contours are shown in Fig. 10. Thus it is seen that  $D \rightarrow K^\pm \pi^\mp \pi^0$  is highly coherent, whereas the indications are that this is not so for  $D \rightarrow K^\pm \pi^\mp \pi^+ \pi^-$ . Interesting results are also obtained for the auxiliary parameters in the fit, where in some cases small but significant improvements are found with respect to the external constraints. For example the fitted value of  $\delta_D^{K\pi}$  is  $(-151.5_{-9.5}^{+9.6})^\circ$  to be compared with the applied constraint of  $(-157.5_{-11.0}^{+10.4})^\circ$ . This sensitivity arises from the importance of the like-sign  $K\pi$  tags in the analysis. A relative 10% improvement is also found in the knowledge of  $y$ , with the fit returning a value of  $0.81 \pm 0.16\%$ , to be compared with the applied constraint of  $0.76 \pm 0.18\%$ .

### Impact on $\gamma$ determination

A study has been made within LHCb to assess the importance of the CLEO-c  $D \rightarrow K(n)\pi$  results on the  $\gamma$  measurement [2]. A standalone simulation study has been made in which the precision on  $\gamma$  is determined from a simultaneous analysis of  $B \rightarrow DK$  events using both  $K^\pm \pi^\mp$  and  $K^\pm \pi^\mp \pi^+ \pi^-$  as  $D$ -decay modes. The simulated events are generated with the  $D$ -decay parameters set to the central values of the CLEO-c analysis. In addition to  $\gamma$ , the fit also returns  $r_B$ , the  $B$ - and  $D$ -meson strong phases, and the coherence factors. The assumed sample

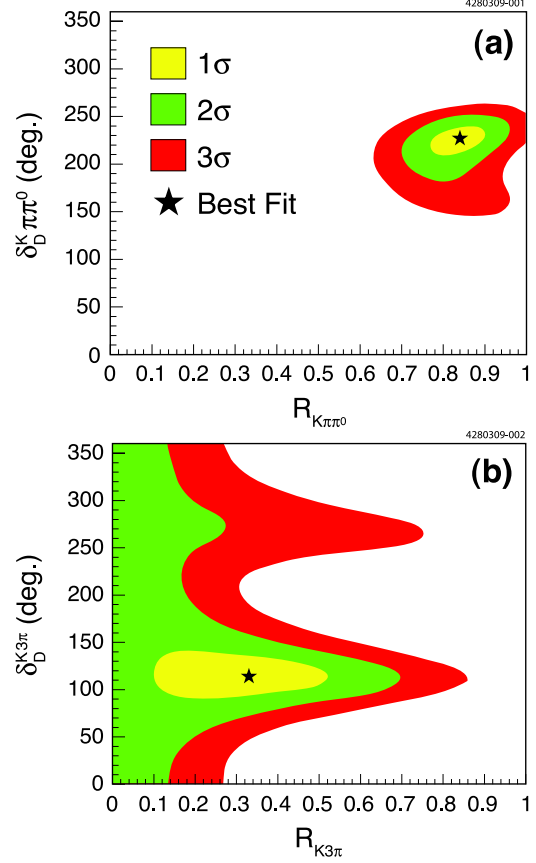


Figure 10: CLEO-c results for the coherence factor and mean strong phase difference for  $D \rightarrow K^\pm \pi^\mp \pi^0$  (a) and  $D \rightarrow K^\pm \pi^\mp \pi^+ \pi^-$  (b).

size corresponds to one nominal year ( $2 \text{ fb}^{-1}$ ) of data. The results are compared between the case where no external knowledge is assumed, and the case where the CLEO-c results for  $\delta_D^{K\pi}$ ,  $R_{K3\pi}$  and  $\delta_D^{K3\pi}$  are applied as external constraints in the fit.

The exact results of the study vary with the assumed value of the parameters, but in general a significant improvement in the precision on  $\gamma$  is observed when the CLEO-c constraints are used, similar to that which would come about from a doubling of the LHCb dataset. The impact of the  $D \rightarrow K^\pm \pi^\mp$  and the  $D \rightarrow K^\pm \pi^\mp \pi^+ \pi^-$  constraints are found to be similar. At first sight the importance of the  $D \rightarrow K^\pm \pi^\mp \pi^+ \pi^-$  events in the analysis is unexpected, given the low value of the coherence. This effect can be understood by inspecting Eqn. 9 and considering the limit when  $R_{K3\pi} \rightarrow 0$ . In this case the observed decay rate in the suppressed  $D \rightarrow K^\pm \pi^\mp \pi^+ \pi^-$  mode allows  $r_B$  to be determined, which then benefits the  $\gamma$  extraction from the simultaneous  $D \rightarrow K^\pm \pi^\mp$  analysis.

The mode  $D \rightarrow K^\pm \pi^\mp \pi^0$  has not yet been included in the LHCb ADS analysis, but it is anticipated that here also the CLEO-c constraints will be helpful in improving the overall  $\gamma$  sensitivity.

## Summary and prospects

CLEO-c analyses have been published which determine  $D$ -decay parameters in the modes  $D \rightarrow K_S^0 \pi^+ \pi^-$ ,  $D \rightarrow K^\pm \pi^\mp$ ,  $D \rightarrow K^\pm \pi^\mp \pi^+ \pi^-$  and  $D \rightarrow K^\pm \pi^\mp \pi^0$ . All these studies rely on the quantum-correlated nature of the  $D - \bar{D}$  pair in  $\psi(3770)$  decays. The results are found to have significant consequences for the measurement of  $\gamma$  in  $B \rightarrow DK$  decays, allowing for both an improvement in overall precision and the removal of model dependence in the analyses. Results are anticipated soon in the mode  $D \rightarrow K_S^0 K^+ K^-$ . Work is also underway to extend the  $D \rightarrow K^\pm \pi^\mp$  analysis to the full  $818 \text{ fb}^{-1}$  dataset, and to provide further results in  $D \rightarrow K_S^0 \pi^+ \pi^-$  for alternative choices of binnings.

There exist other channels which are potentially useful in the  $B \rightarrow DK$  analysis and so could benefit from measurements of their decay properties in quantum correlated events. These include  $D \rightarrow K^+ K^- \pi^+ \pi^-$ ,  $D \rightarrow K_S^0 K^\pm \pi^\mp$  and  $D \rightarrow K_S^0 \pi^+ \pi^- \pi^0$ .

The studies reported here would benefit greatly from the increase in  $\psi(3770)$  statistics which could be collected by the BES-III experiment. For this reason a significant open charm programme at BES-III is to be encouraged.

## Acknowledgements

I am grateful to Jim Libby and other CLEO-c colleagues for useful discussions in preparing this review.

## References

- [1] J. Charles *et al.* (CKMfitter group), Eur. Phys. J. **C 41** (2005) 1, updated results and plots available at : <http://ckmfitter.in2p3.fr/>.
- [2] K. Akiba *et al.*, *Determination of the CKM-angle  $\gamma$  with tree-level processes at LHCb*, LHCb-2008-031.
- [3] Y. Wang, *Status of BES-III*, these proceedings.
- [4] B. Aubert *et al.* (BABAR Collaboration), Phys. Rev. **D 78** (2008) 034023.
- [5] K. Abe *et al.* (Belle Collaboration), arXiv:0803.3375 [hep-ex].
- [6] Review on Dalitz plot formalism in [20].
- [7] E.P. Wigner, Phys. Rev. **70** (1946) 15; S.U. Cheung *et al.* Ann. Phys. (Paris) **507** (1995) 404; I.J.R. Aitchison, Nucl. Phys. **A 189** (1972) 417.
- [8] D. Aston *et al.* (LASS Collaboration), Nucl. Phys. J. **B 296** (1988) 493.
- [9] V. Gibson, C. Lazzeroni and J. Libby, *Measuring  $\gamma$  at LHCb with  $B^\pm \rightarrow D^0/\bar{D}^0(K_S^0 \pi^+ \pi^-)K$  decays*, LHCb-2007-048.
- [10] A. Giri *et al.*, Phys. Rev. **D 68** (2003) 054018.
- [11] A. Bondar and A. Poluektov, Eur. Phys. J **C 55** (2008) 51; A. Bondar and A. Poluektov, Eur. Phys. J **C 47** (2006) 347.
- [12] R.A. Briere *et al.* (CLEO Collaboration), Phys. Rev. **D 80** (2009) 032002.
- [13] S. Ricciardi, *Quantum Correlated D Decays at CLEO-c*, Europhysics Conference on High Energy Physics, 16-22 July 2009, Krakow, Poland.
- [14] D. Atwood, I. Dunietz and A. Soni, Phys. Rev. Lett. **78** (1997) 3257; D. Atwood, I. Dunietz and A. Soni, Phys. Rev. **D 63** (2001) 036005.
- [15] D. Atwood and A. Soni, Phys. Rev. **D 68** (2003) 033003.
- [16] D.M. Asner *et al.* (CLEO Collaboration), Phys. Rev. **D 78** (2008) 012001; J.L. Rosner *et al.* (CLEO Collaboration), Phys. Rev. Lett. **100** (2008) 221801.
- [17] The Heavy Flavor Averaging Group (HFAG), <http://www.slac.stanford.edu/xorg/hfag>.
- [18] P. Naik, *D mixing at CLEO-c*, these proceedings.
- [19] N. Lowrey *et al.* (CLEO Collaboration), Phys. Rev. **D 80** (2009) 031105 (R).
- [20] C. Amsler *et al.* (Particle Data Group), Phys. Lett. **B 667** (2008) 1.